JOURNAL OF SOLID STATE CHEMISTRY 5, 266–275 (1972)

Rare Earth Silicates with the Apatite Structure

J. FELSCHE

Institut für Kristallographie und Petrographie der ETH, Zürich, Switzerland

Received September 30, 1971

Complete series of apatite like compounds $RE_{9.33}\square_{0.67}[SiO_4]_6O_2$, $LiRE_9[SiO_4]_6O_2$, $NaRE_9[SiO_4]_6O_2$ have been synthesized with RE: La → Lu. From anisotropic response of the unit-cell dimensions suggestions are made on the cation distribution on the (4*f*)- and (6*h*)-lattice sites. Crystal data on (Mg, Ca, Sr, Ba)$_2RE_8[SiO_4]_6O_2$ and (Ca, Sr, Ba, Pb)$_4RE_6[SiO_4]_6(OH)_2$ are also included in the structural discussion.

Introduction

This study is mainly based on the recent comprehensive results on silicate hydroxy-apatites and oxyapatite compounds given by Ito (*1*) and as well on the structure investigations on the cation deficient type of silicate apatite, $RE_{9.33}\square_{0.67}[SiO_4]_6O_2$ as reported by Kuzmin and Belov (*2*) and Smolin and Shepelev (*3*) for La, Sm and Gd, respectively. A comprehensive survey of the related literature has been presented in (*1*). Therefore it will be omitted at this place but it will be referred to in single cases of interest during the discussion on our own data. However, it seems worthwhile for the outline of this paper to give the general impression from the numerous apatite papers published recently on multivalent charge couple substitution. It is likely to be very tempting during synthetic experiments especially for the various apatite like compounds to establish new chemical formulas from the overall chemical data or even from the composition of the starting material as soon as the X-ray examination provides the apatite diffraction pattern. This happens especially since the apatite structure type is known to be extremely tolerant to any type of charge coupled cation and anion substitution as well as to cation and probably also to anion deficiency. It should be realized, however, that just in the case of any complicated stoichiometry (solid solution, mixed phases of different degree of crystallinity) reliable data can only be obtained by analysis of single crystals. In cases, where the size of the crystals drops below the resolution given by the common electron microprobe technique (1–10 μ) for chemical data or below the 1000 Å limit for X-ray powder work or below the 0.1-mm limit for X-ray single crystal study one takes the risk to establish the wrong chemical formula.

In extension of the critical remarks given recently on this problem (*23*), it should be mentioned, however, that the best results in the field of cation–anion distribution and deficiency will be achieved by correlation of qualified analytical data from chemical analysis, simultaneous DTA/TGA, density measurement, spectroscopic methods and finally structure analysis of single crystals. The latter is likely the most efficient method for this problem, although it has been applied only once in the last years for the determination of the (4*f*) cation deficient type of apatite. Data on cation substitution presented in this paper were obtained in agreement with the outline given above. The structural interpretation of the crystal data is of the preliminary state. Final conclusions on ion distribution will be drawn from structure analysis which will follow this study.

Experimental

Complete series of compounds $RE_{9.33}[SiO_4]_6O_2$, $Li\,RE_9[SiO_4]_6O_2$ and $Na\,RE_9[SiO_4]_6O_2$ were synthesized by solid state reaction. Pellets containing the corresponding oxide/salt mixtures $7RE_2O_3 \cdot 9SiO_2$, $Li_2CO_3 \cdot 9RE_2O_3 \cdot 12SiO_2$ and $Na_2CO_3 \cdot 9RE_2O_3 \cdot 12SiO_2$ were pressed with 200 kg/cm^2 and annealed at different temperatures

in the range of 1000–1900°C for 24 hr after presintering at 900°C.

Up to 1600°C the heating experiments were carried out in air in a resistance oven with superkanthal heating elements; above 1600°C, HF equipment was used with specimens under argon packed in Ir foil.

The chemical composition of synthesized compounds was confirmed by electron microprobe data on single crystals 0.01–0.20 mm in size. The alkali concentration was determined by flame photometry.

X-Ray examination was carried out on single crystals of most of the compounds as far as available from the synthesis. Space group symmetry was controlled by Mo$K\alpha$ precession photographs. Guinier photographs were taken from all synthesized specimens. Sets of *d*-spacings for the least-squares refinement of the unit-cell dimensions were obtained from Guinier–Jagodzinski photographs taken with the camera in −45° asymmetric position using Fe$K\alpha_1$ radiation and Si as a standard.

For the starting mixtures, 99.99% rare earth oxides were used from Auer–Remy, Hamburg and 99.99% SiO_2 (Kieselguhr), Li_2CO_3 and Na_2CO_3 from Merck, Darmstadt. The heating experiments were controlled by simultaneous DTA/TGA runs on a "Mettler Thermoanalyzer." A mass-spectrometer (MAT-GD150) connected to the reaction chamber registered the evaporized CO_2 from the reaction $(Na,Li)_2CO_3 \rightarrow (Li,Na)_2O + CO_2\uparrow$. In case of multivalent rare earths the appearance of gaseous oxygen has been immediately recognized during the reduction of tetravalent Ce, Pr, Tb in CeO_2, Pr_6O_{11}, Tb_6O_{11} to the corresponding sesquioxide forms, and of trivalent Eu in Eu_2O_3 to 2EuO at the formation of $Eu_2^{2+}Eu_8^{3+}[SiO_4]_6O_2$. No alkali evaporization was observed below 1150°C.

Results and Discussion

Compounds $RE_{9.33}\square_{0.67}[SiO_4]_6O_2$ were successfully prepared in 50–100°C step-by-step heating experiments from 1000 to 1900°C. Congruent melting was observed at temperatures 1950–1850 ± 30°C slightly decreasing with increasing atomic numbers of the rare earths La → Gd. This is in agreement with former results on the so-called 2:3 compounds on various RE_2O_3–SiO_2 phase diagram investigations (*4–8*). Tb-, Dy-, Ho-specimens were always found accompanied by 10–20 mol % of the disilicate polymorphs type B, D, E (*9*). However, the corresponding excess of RE_2O_3 could not be observed in any of the sesquioxide forms on the Guinier-photographs neither in one of the forms of $RE_2[SiO_4]O$ (*10–12*). The $7RE_2O_3 \cdot 9SiO_2$ composition of the smaller rare earths (Ho), Er, Tm, Yb, Lu (Ho: $T > 1550$°C) on the contrary contained almost less than 20 mol % of the apatite phase but corresponding $RE_2[SiO_4]O$ (*10*) and polymorphic disilicate phases type C and D (*9*) due to

$$5(7RE_2O_3 + 9SiO_2) \rightarrow 3(5RE_2[SiO_4]O + 2RE_2[Si_2O_7]) + RE_{9.33}\square_{0.67}[SiO_4]_6O_2.$$

The single-crystal microprobe data taken from 10–200 μ particles of all the 7:9 compounds showed variations of $\leqslant 0.2$% about the theoretical RE:Si atomic ratio of 1.555. One exception was given by the Eu-apatite phase. From Eu:Si = 1.570 ± 0.002 and the corresponding distinct value of the c_0-dimension an appreciable amount of Eu^{2+} is indicated to be present in the structure; thus representing solid solution between the pure trivalent Eu-apatite and the mixed valency compound $Eu_2^{2+}Eu_8^{3+}[SiO_4]_6O_2$. The latter has been synthesized as well from a 5:6 oxide mixture under reducing atmosphere (formiergas H_2/N_2). The experiment was controlled in a simultaneous TGA/DTA run. The partial reduction of $Eu^{3+} \rightarrow Eu^{2+}$ corresponding to 0.78% loss of the total starting weight occurs at 1050°C: $5Eu_2O_3 + 6SiO_2 \rightarrow$

$$Eu_2^{2+}Eu_8^{3+}[SiO_4]_6O_2 + 0.5O_2\uparrow.$$

The microprobe examination carried out on crystals with 0.05 mm in diameter gave RE:Si = 1.661 ± 0.002 which meets the theoretical value for the given formula of 1.666 quite well.

Compounds Li- and $NaRE_9[SiO_4]_6O_2$ were prepared at 1100°C. As compared with the binary RE silicate apatite phases, an assemblage with other RE silicates has mostly not been observed besides with the smallest rare earths Yb and Lu, which gave corresponding mixtures. The Ce-analogs had to be synthesized under reducing atmosphere because CeO_2 admixtures were found on quenching in air. Pr- and Tb-compounds of Li and Na could be synthesized in air without reoxidation.

The RE:Si atomic ratio of 1.500 with variations ±0.004 has been confirmed for several compounds representing the complete RE series.

The corresponding Li and Na concentration derived from the flame-photometric data is good agreement with the given formula.

At temperatures > 1150°C an appreciable loss of weight of both the alkali compounds was observed on the thermobalance. This is due to the increasing vaporization of the alkalies at elevated temperatures. The compounds were found to decompose to their alkali free analogs.

Single-crystal X-ray examination of several RE- and alkali RE-analogs confirmed the space group $P6_3/m$ ($P6_3$) for the complete series of binary and ternary rare earth compounds. Reflections $00l$ and hkl with $l \neq 2n$ were found absent in the case of hkl, if $h - k = 3n$ on Mo$K\alpha$-precession photographs. Powder diffraction patterns could be entirely interpreted in terms of the known apatite crystal data and also in the case of mixed phases consisting of apatite, polymorphic disilicate and oxyorthosilicates. Refined values of the unit-cell dimensions are listed in Table I. The lattice constants of $Eu_2^{2+}Eu_8^{3+}[SiO_4]_6O_2$ with e.s.d.'s as given in Table I are: $a_0 = 9.470$ Å, $c_0 = 6.998$ Å, $V = 542.8$ Å^3.

Since the *cation deficient oxyapatite structure* has been established by structure analysis for La, Sm (*2*) and Gd (*3*), the mol composition $7RE_2O_3 \cdot 9SiO_2$ of the crystals might be described more efficiently in terms of the true unit-cell content, $(RE_{3.33}\square_{0.67})^{[9]}RE_6^{[7]}[Si_4^{[4]}O_4^{[4]}]_6O_2^{[3]}$. Numbers in square brackets at the upper right of the elements give the coordination number (CN). The main structural units are shown in Fig. 1 for the Gd analog (*3*). With an error $\leqslant 1\%$ from the refinement of the multiplicity of Gd it has been shown that 2/3 cation holes per cell are statistically distributed on the ($4f$) lattice sites. This special position is surrounded by 9 oxygens, which are all silicon bonded. The ($4f$) position with the mean Gd–O distance of 2.53 Å offers the larger space for cation substitution as compared to the 7-fold coordinated ($6h$) lattice site with the average Gd–O distance of 2.41 Å. Another interesting feature which concerns the ($6h$) "channel" position is the extremely short distance of 2.23 Å with the "free" oxygen on the special position 0, 0, $\frac{1}{4}$; 0, 0, $\frac{3}{4}$ along the 6_3-axis. This distance, which is considerably smaller than the sum of the ionic radii indicates the strong polarizing forces of the rare earth cations on the oxygen, which is not silicon bonded.

The experimental data on the Gd apatite structure (*3*) served as a base to determine the *effective ionic radii of the complete series of* RE^{3+} *cations* in this structure type from a plot, cell volume *vs.* r^3. Regarding that the effective radius of any ion depends on both the coordination numbers of the cation and anion, the mean RE^{3+} radii in the apatite structure have been determined from the 7- and 9-fold coordinated

TABLE I

UNIT-CELL DIMENSIONS OF COMPOUNDS $RE_{9.33}\square_{0.67}[SiO_4]_6O_2$, $LiRE_9[SiO_4]_6O_2$ AND $NaRE_9[SiO_4]_6O_2$ WITH RE: La → Lu[a]

RE	$RE_{9.33}\square_{0.67}[SiO_4]_6O_2$			$LiRE_9[SiO_4]_6O_2$			$NaRE_9[SiO_4]_6O_2$		
	a_0 (Å)	c_0 (Å)	V (Å^3)	a_0 (Å)	c_0 (Å)	V (Å^3)	a_0 (Å)	c_0 (Å)	V (Å^3)
La	9.713	7.194	587.8	9.681	7.160	581.2	9.687	7.180	583.5
Ce	9.657	7.121	575.1	9.623	7.091	568.7	9.628	7.117	571.3
Pr	9.607	7.073	565.3	9.575	7.040	558.8	9.580	7.080	562.6
Nd	9.563	7.029	556.9	9.529	6.994	550.1	9.535	7.027	553.4
Sm	9.493	6.946	542.0	9.464	6.918	536.6	9.472	6.943	539.6
Eu	9.472	6.905	536.6	9.437	6.876	530.3	9.456	6.912	535.2
Gd	9.431	6.873	529.4	9.413	6.852	525.8	9.419	6.878	528.4
Tb	9.401	6.825	522.4	9.381	6.803	522.0	9.390	6.840	522.2
Dy	9.373	6.784	516.2	9.362	6.769	513.9	9.362	6.800	516.2
Ho	9.346	6.744	510.3	9.337	6.736	508.6	9.337	6.760	510.4
Er	9.324	6.686	503.4	9.316	6.696	503.3	9.321	6.728	506.2
Tm	9.300	6.666	499.3	9.301	6.672	499.8	9.310	6.688	502.0
Yb	9.275	6.636	494.4	9.270	6.637	493.8	9.300	6.661	498.8
Lu	9.260	6.621	491.6	9.265	6.615	490.9	9.290	6.635	495.9

[a] Refined values from Guinier Fe$K\alpha_1$-data have ESD's of $\sigma(a_0) = 0.002$ and $\sigma(c_0) = 0.001$ Å.

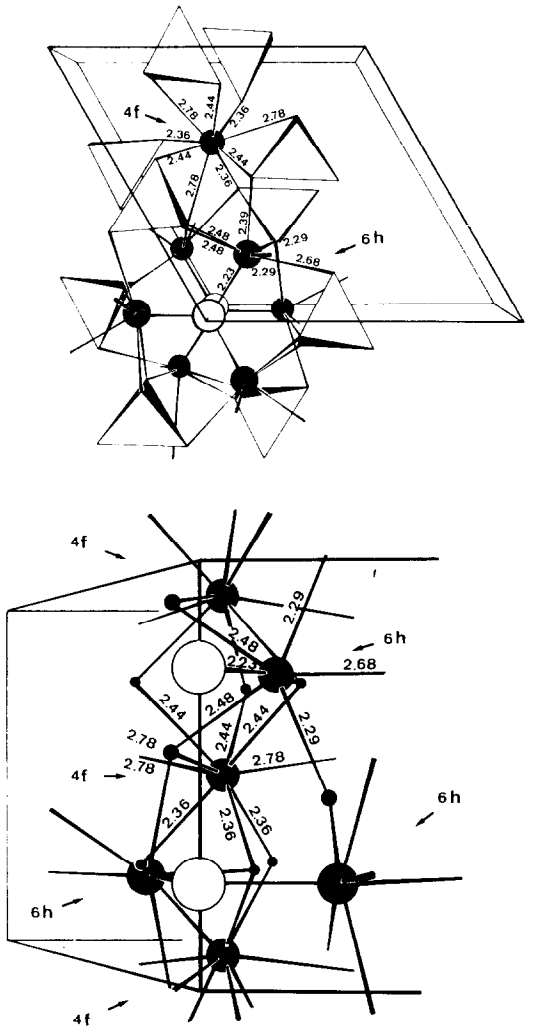

FIG. 1. Perspective view on the structure of rare earth silicate oxyapatites $(RE_{3.33}\square_{0.67})RE_6[SiO_4]_6O_2$ along [001] and [100]. Interatomic distances from data on the Gd-analog (*3*) with ESD's ranging from 0.002 to 0.008 Å. Black balls: rare earths on the special positions (4*f*) and (6*h*); white balls: "free" not silicon bonded oxygen; solid $[SiO_4]$ tetrahedra.

cations in the following way. The refined values of the Gd–O distances show ESD's in the order of 0.008 Å corresponding to an overall *R*-value for the structure of 6.5%. The average Gd–O distances in the (4*f*) polyhedron with CN 9 and in the (6*h*) polyhedron with the CN 7 are 2.53 and 2.40 Å, respectively. The 24 silicon-bonded oxygens per unit-cell are surrounded by 4 cations, whereas the 2 "free" oxygens have 3 RE neighbors. Thus with the average O^{2-}-radius of 1.38 Å (*13*), the effective Gd^{3+}-(4*f*) and Gd^{3+}-(6*h*) ionic radii are 1.15 and 1.02 Å. From these data the weighted mean value of the Gd^{3+} ionic radius in the apatite structure has been determined to 1.08 Å. In Fig. 2 the plot cell volume *vs.* r^3 is shown. The relative scale of the trivalent rare earth radii has been maintained from the known RE^{3+} series with CN 6 (*13*). However, the complete set has been shifted to the determined effective ionic radius of $Gd^{3+} = 1.08$ Å. The correlation with the other rare earths is quite linear. The La^{3+}- and Ce^{3+}-values might have to be corrected to slightly smaller values of 1.19 and 1.17 Å. The special situation of the Eu-analog, which arises from probably mixed Eu^{2+}–Eu^{3+} valency is no point of interest at this place of the discussion.

The apatite structure shows an anisotropic response on substitution with the various rare earths which cover a range of ionic radii from 1.20 to 0.99 Å for La → Lu. As can be seen from the plot a_0 and c_0 *vs.* *r* in Fig. 3 the variation of the c_0 axis is much more distinct than it is of the a_0 axis. In respect to the La analog, the structure of, e.g., Lu-apatite shows a shrinkage of 9.6% along the *c*-direction as compared to 4.7% along a_0. This is best understood in terms of the Gd–O interatomic distances given in Fig. 1. The shortest Gd–O bonds are directed closely along [001] from both the cation positions (4*f*) and (6*h*).

Another interesting feature from Fig. 3 are the changes in slope and intersections at different positions along a_0 and c_0. The c_0-axis indicates three groups Lu–Er, Ho–Nd, and Nd–La as commonly known from rare earth chemistry, whereas a_0 shows one intersection between Gd and Eu only.

In Fig. 3 some additional data from the literature have been compiled concerning the binary compound $7RE_2O_3 \cdot 9SiO_2$ and the ternary alkali rare earth phase. Most of the given crystal data show only poor agreement with our own values of the apatite cell dimensions. The differences might depend on the X-ray diffraction technique used and/or the way of evaluation of the experimental data and thus on the different accuracy of the results. However, in most cases, ESD's are not even given. On the other hand, traces of the employed flux (e.g., alkalifluorides, bismuth oxide) could be accommodated into the structure and thus be responsible for the variation of the cell-dimensions; or even admixtures of other rare earths to the starting RE_2O_3. The largest deviations from the data in Fig. 3 are given by the La- and Sm-analogs from Ref. (*2*).

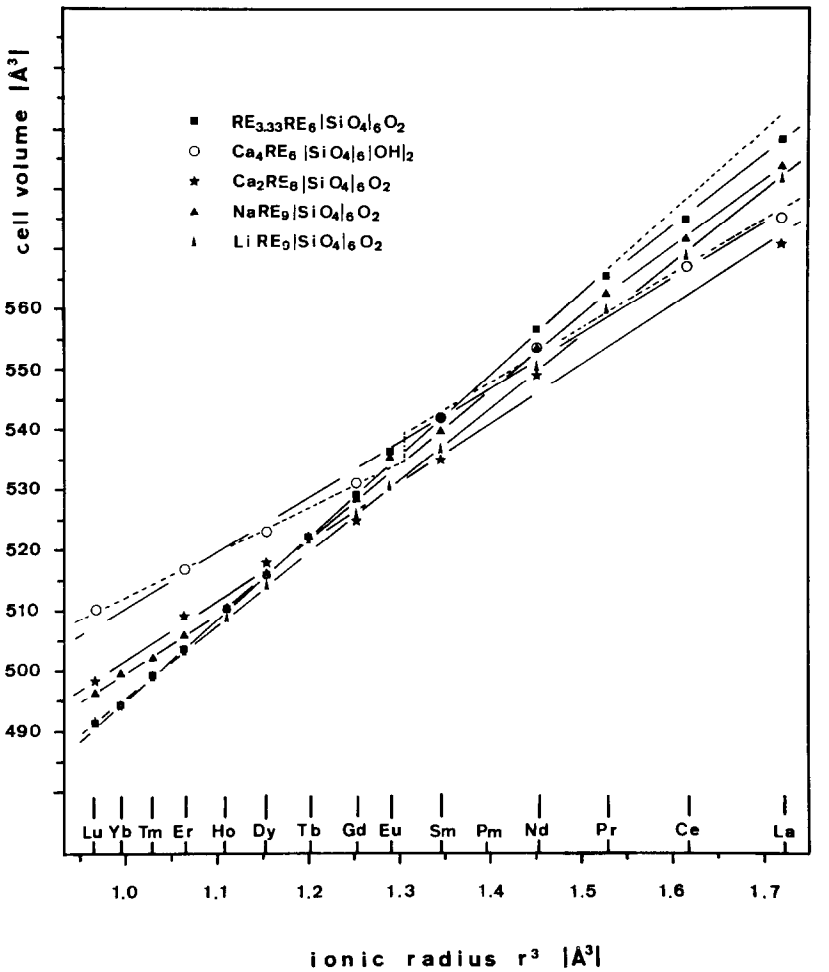

FIG. 2. Cell volume V *vs.* r^3 (RE^{3+}-ionic radii) of rare earth silicate apatites showing different mixed cation ratios 1:9, 2:8, 4:6 as compared to the binary cation deficient compound $(RE_{3.33}\square_{0.67})RE_6[SiO_4]_6O_2$. Data of $Ca_2RE_8[SiO_4]_6O_2$ and $Ca_4RE_6[SiO_4]_6O_2$ from (*1*). ESD's of the cell volume are ≤ height of the symbols.

The values for a_0 and c_0 are 0.17 and 0.07 Å smaller, far beyond the probable ESD's (not given). This fact lacks any reasonable explanation especially because the structure analysis, which have been carried out with these crystals gave the same result of a cation deficient (4*f*) position as described for the Gd-apatite (*3*). Since the data from Ref. (*3*) show a better general agreement with the data, the structure data for La and Sm (*2*) have not been referred to for the evaluation of the effective ionic radii. The different agreement with the various data from the same source as the Gd-analog (*3*) might be due to the different methods employed for the synthesis of the crystals.

The wide range of stability of the apatite phase in the binary system RE_2O_3–SiO_2 is best illustrated by the fact that values obtained from Refs. (*15*) and (*16*) were actually given for compositions $1RE_2O_3 \cdot 1SiO_2$ and from Refs. (*8*, *10*, *17*, *18*) for $2RE_2O_3 \cdot 3SiO_2$. Some attempts to identify the apatite cell dimensions from the unindexed powder data given in (*4–7*) were not successful because of the poor resolution and the obvious mixed phase character of most of the listed diffraction patterns.

So far there does not exist any reliable experimental result for the deficient apatite type $La_{8.67}(SiO_4)_6O$ as described in Ref. (*19*), for which cell dimensions are given almost identical with those of the common $7La_2O_3 \cdot 9SiO_2$ type. Also in the ternary system $Li_2O \cdot RE_2O_3 \cdot SiO_2$, the Li–$RE_9$ apatite seem to exhibit a large area of stability. This is suggested at least by the crystal

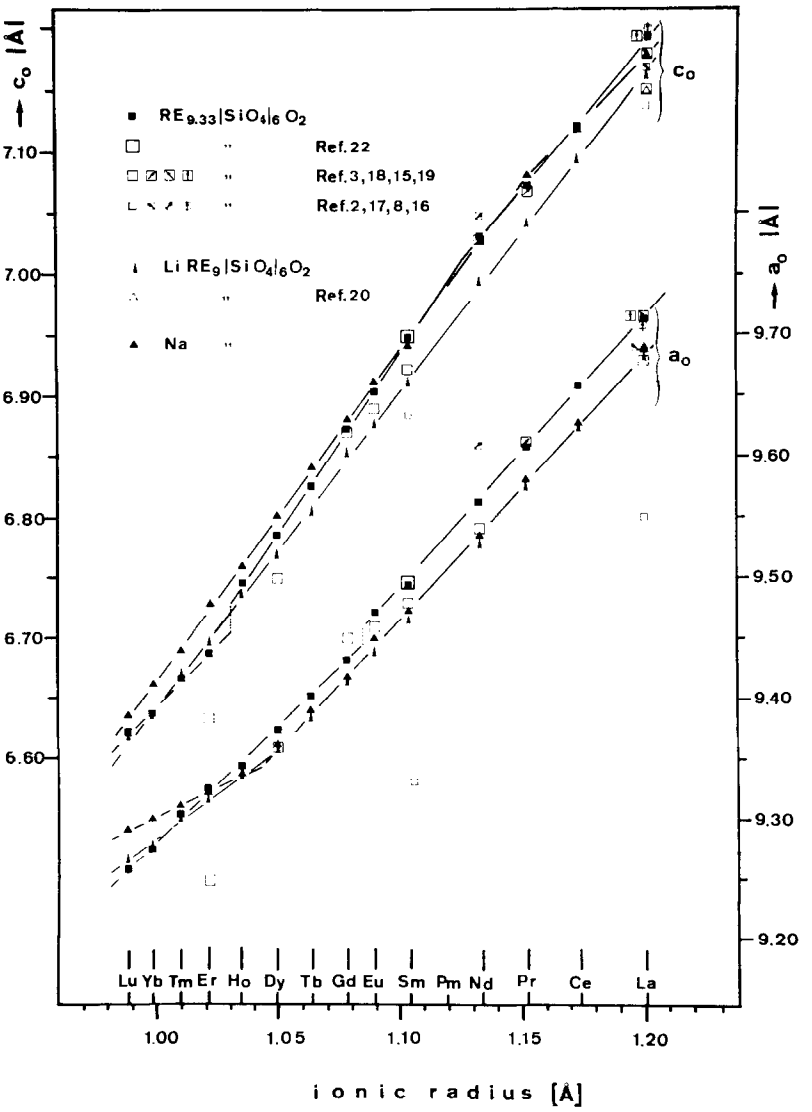

FIG. 3. Cell dimensions c_0 and a_0 *vs.* r (RE^{3+}) of binary rare earth and alkali rare earth silicate oxyapatites. Data from different sources [Ref. (n)] and our own experiments (Table I). ESD's are unknown for values from Refs. (*2*, *8*, *15–17*, *20*); ESD's of 0.003 to 0.002 Å are given in Refs. (*18*, *19*, *22*), of 0.01 Å in Ref. (*3*).

data $a = 9.69$ Å, $c = 7.15$ Å given for $LiLaSiO_4$ (*20*), which indicates the known apatite phase rather than "a new family of lanthanide compounds" with RE = La → Dy.

With *mixed cation substitution* the distinct anisotropic behavior and formation of subgroup along the RE series changes or vanishes completely. In Fig. 2 several representatives of different stoichiometry 1:9, 2:8 and 4:6 have been compiled. The general result is the expected decreasing slope of the cell volume *vs.* r^3 (RE^{3+}) of compounds with increasing amount of foreign (not RE) cations.

Compounds $LiRE_9[SiO_4]_6O_2$ show even a more ideal linear relationship between cell volume and cubic RE^{3+}-radius in Fig. 2 than the pure RE-apatites. The sodium analog, however, shows a change in slope beyond Ho. It is interesting to see in Fig. 3 that the pronounced breaks in the curves a_0 and c_0 *vs.* r of the pure RE apatites, which depend on the atomic RE characteristics, are vanishing on introduction of only one small

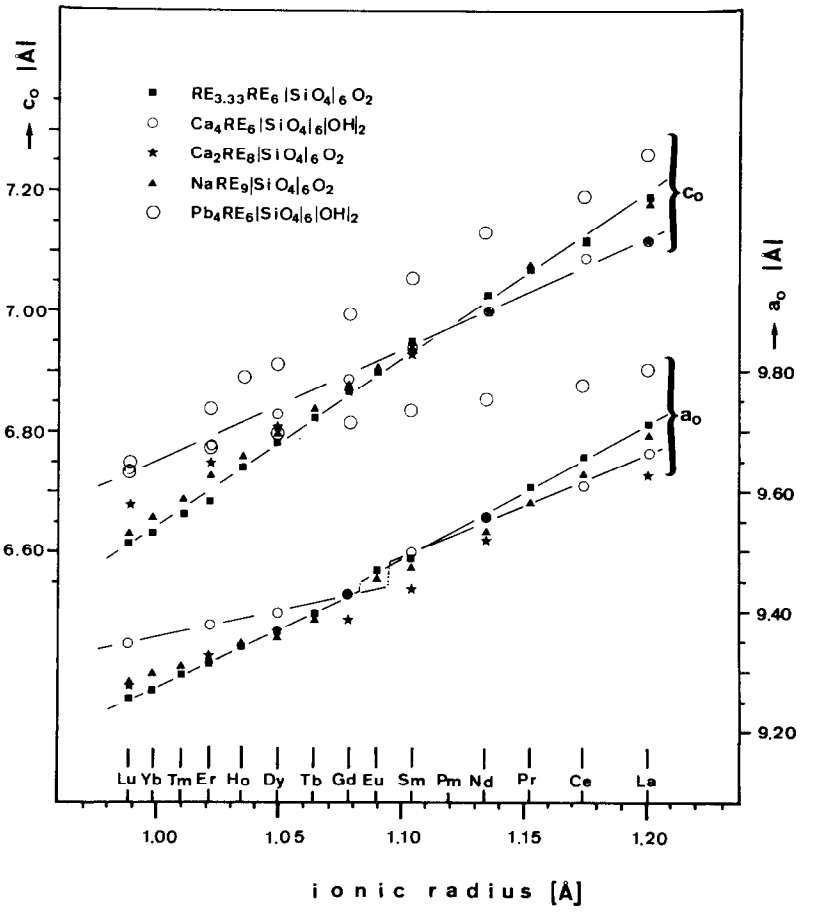

FIG. 4. Survey of cell dimensions a_0 and c_0 *vs.* r (RE^{3+}) of some representative RE silicate apatites showing different mixed cation ratios 1:9, 2:8, 4:6 as compared to the binary cation deficient apatite $(RE_{3.33}\square_{0.67})RE_6[SiO_4]_6O_2$. Data for Ca- and Pn-analogs from Ref. (*1*) with ESD's of 0.01 Å (private communication).

but different cation per cell. Apparently from this moderator function of the alkali atom the c_0-dimension of the $LiRE_9$-apatites varies linearly with r along the complete RE-series, no subdivision shows up. A change in the slope of a_0, however, is indicated at Ho.

This change in the slope at Ho is even more pronounced with the compounds $NaRE_9[SiO_4]_6O_2$ while their absolute a_0-values beyond Dy with the larger rare earths are about the same. c_0, however, is generally about $\leqslant 0.04$ Å larger than in Li-apatite. For La to Gd, c_0 of the sodium analog meets about the data of the pure RE-apatite whereas the c_0 values of the smaller $NaRE_9$-apatites are significantly larger.

Regarding that the single alkali atom per cell replaces formally the combination $(\frac{1}{3}RE + \frac{2}{3}\square)^{1+}$ it seems likely that the small alkali prefers the smaller volume of the (6*h*) position in a statistical distribution. This is also suggested by the significant change in slope of a_0 *vs.* r in Fig. 3. It occurs at a place where the Na^{1+}-radius becomes competitive to the rare earths around Ho–Dy. It is apparent from Fig. 1 that the variation of the a_0 axis should depend mostly on the substitution of the (6*h*) lattice site rather than of the (4*f*) one. This is because the (6*h*) position has the more tight bonds in directions [*hk*0] (2.23, 2.39, and 2.68 Å) than the (4*f*) cation with three 2.78 Å Gd–O distances.

In order to follow the correlation between cation distribution and variation of cell dimensions also for 2:8 and 4:6 mixed cation apatites the crystal data given for these compounds in Ref. (*1*) will be discussed. Since the standard deviations of these values with 0.01 Å (private communication) are larger than of the own data ($\leqslant .002$ Å) the scale for a_0 and c_0 in Figs. *4–6*

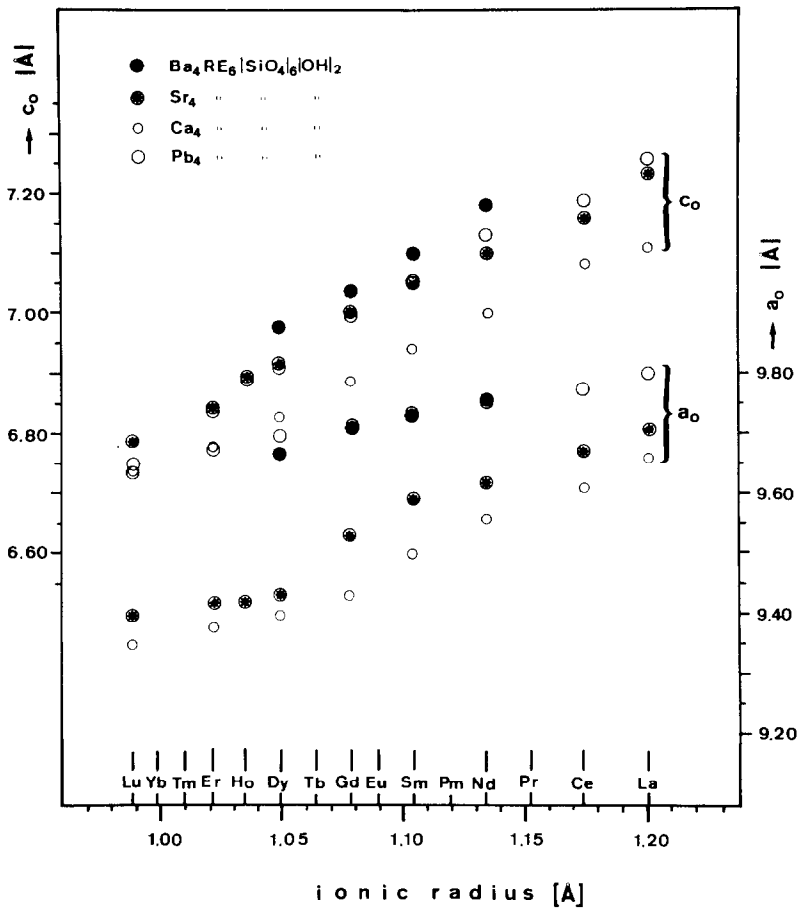

FIG. 5. Cell dimensions a_0 and c_0 *vs.* r (RE^{3+}) of RE silicate hydroxyapatites with mixed cation ratio 4:9. Data from Ref. (*1*), with ESD's 0.01 Å (private communication).

has been changed in order to give a comprehensive representation.

In compounds $Me_4RE_6[SiO_4]_6(OH)_2$ with Me: Mg, Ca, Sr, Ba, Pb, Cd, Mn of mixed cation ratio 4:6 the two "free" oxygens located in the main channels of the structure are replaced by OH-groups. However, the presence of OH-groups causes apparently only slightly different interatomic distances within the (6*h*) coordination polyhedron as compared to the values known from the Gd-oxyapatite (*3*). This is suggested from structure data on the synthetic calcium-hydroxyapatite (*21*). The 4:6 apatite compounds seem worthwhile to be introduced into this discussion because their mixed cation ratio meets exactly the ratio of the symmetry equivalent positions (4*f*):(6*h*) per cell. Therefore, order–disorder on these lattice sites should show up more easily here than in any of the other mixed cation compounds. From the variation of the cell dimensions on substitution of cations of different size into both the positions (4*f*) and (6*h*), distinct effects should be expected. The results as shown for the Ca-, Sr-, Ba-, Pb-analogs in Fig. 5 are less unambiguous than should be anticipated from the corresponding statement in (*17*). There from comparison of 4 relative X-ray intensities it had been concluded on a random distribution of the cations on (4*f*) and (6*h*) lattice sites.

Roughly the following points from Fig. 5 seem worthwhile to be mentioned. The largest type of Me-cation substituted is Ba^{2+} with $r = 1.39$ Å (CN 7) and $r = 1.47$ Å (CN 9) followed in size by Pb^{2+} with $r = 1.25$ Å and $r = 1.33$ Å, respectively (*13*). The almost identical values of a_0 and the significant larger c_0 cell-dimensions suggest the cations Ba^{2+} and Pb^{2+} to be present in the (4*f*)

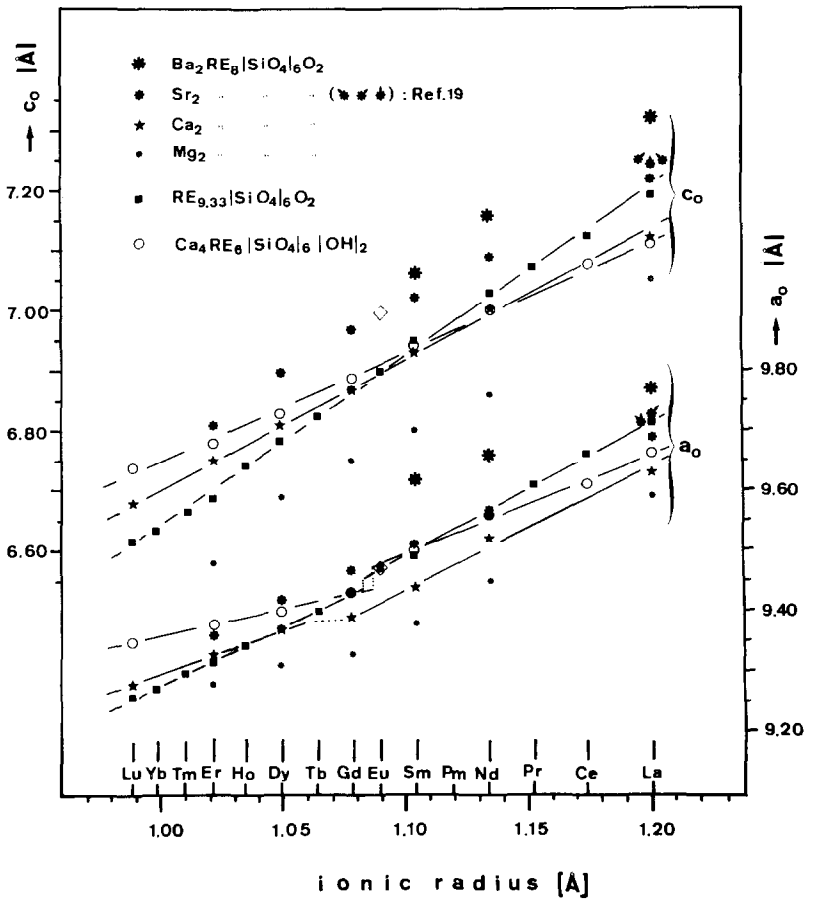

FIG. 6. Cell dimensions a_0 and c_0 *vs.* r (RE^{3+}) of RE silicate oxyapatite with mixed cation ratio 2:8 from Ref. (*1*) with ESD's 0.01 Å (private communication). Compared to the binary RE silicates (our data) and the Ca-hydroxy-apatites with mixed cation ratio 4:6 also from (*1*). The rhombus like symbol represents cell dimensions of $Eu_2^{2+}Eu_8^{3+}[SiO_4]_6O_2$.

position since (4*f*) has been recognized to be most sensitive in the c_0 direction. The next smaller cation Sr^{2+} shows the c_0-dimension of the unit cells to be almost the same as for Pb^{2+} whereas the a_0 values vary by 0.10 to 0.25 Å, the difference increasing with RE atomic numbers. This indicates a change in cation distribution, with Sr^{2+} also present on the "smaller" (6*h*) sites. These were considered above to be mainly responsible for any response of the apatite structure along a_0. The random distribution of Sr^{2+} on (6*h*) and (4*f*) lattice sites yields a similar slope for both the cell dimensions along the RE series up to a critical point. There the Sr^{2+} ionic radius maintains a larger value than the continuously contracting RE^{3+} ions and thus blocks a further shrinking of the (6*h*) sensitive a_0 direction. These critical values are reached around Gd, Tb, Dy for the Sr_4RE_6 apatite as well as for the Ca-analog, which behaves similarly. The blocking of the a_0-axis variation is thus responsible for the break in the corresponding curves of V *vs.* r^3 in Fig. 2.

Oxy-apatite compounds of mixed cation ratio 2:8 show some analogy with the latter ones. Data for $Me_2RE_8[SiO_4]_6O_2$ with Me: Mg, Ca, Sr, Ba from Ref. (*1*) are presented in Fig. 6. The Mg- and Ca-analogs show a corresponding change in slope of a_0 at Gd whereas their c_0-dimension varies quite continuously. This means that Mg and Ca ions are probably also accommodated on (6*h*) sites following the former arguments. Substitution of the larger Sr^{2+} yields a different effect on the structure. a_0 and c_0 values vary similarly over the given range of rare earths La → Er with a slope slightly increasing with the

RE atomic numbers. Hereby a change in cation distribution seems indicated with $(2Sr^{2+} + 2RE^{3+})$ in the larger coordination of (4*f*). This should also be true for the 2:8 analogs of Ba which exists, however, only with the larger rare earths La → Sm. This limit has been found extended to La → Dy for the 4:6 analogs of the Ba-hydroxy-apatites.

In Fig. 6 also some cell dimensions of various mixed (Sr, La)-oxy-apatites are shown from Ref. (*19*). Two different types of deficient apatite structures are described there in addition to the known cation deficient apatite $RE_{9.33}[SiO_4]_6O_2$ by formulas $Sr_2La_{6.67}[SiO_4]_6$, $Sr_3La_6[SiO_4]_6$, $Sr_4La_{5.33}[SiO_4]_6$ (♂) and $Sr_4La_6[SiO_4]_6O$ (♂). No reliable experimental data do exist, however, so far to confirm these types of oxygen deficiency in the silicate apatite structure. As already mentioned for $La_{8.67}[SiO_4]_6O$ in respect to $La_{9.33}[SiO_4]_6O_2$ also, here the given cell dimensions of the various Sr–La-apatites altogether indicate one type of compound to be present only, which is $Sr_2La_8[SiO_4]O_2$ (♂) within the limits of accuracy of the data given in (*1*, *19*).

The conclusion concerning the latter problem is that reliable information on the stoichiometry of these compounds can only be obtained by chemical analysis of a single crystal and (or) a structural investigation of the same crystal. Determination of the ion distribution on different lattice sites should be successful by up-to-date X-ray analysis even for oxygen in respect to the heavy atoms present in the apatite structure. Otherwise neutron-diffraction could help to clarify the problem of partial or complete oxygen deficiency in the main channel of the structure. Application of structure analysis seems also to be necessary to confirm the various indications for different distribution as described in this paper. A series of structure determinations on mixed cation silicate apatites is going to follow this study.

Acknowledgments

The author thanks Prof. F. Laves for his interest in this work, W. Hirsiger for collaboration and helpful assistance and Owens-Illinois, Inc. Toledo, for financial support.

References

1. J. Ito, *Amer. Mineral.* **53**, 890 (1968).
2. E. A. Kuzmin and N. V. Belov, *Dokl. Akad. Nauk SSSR* **165**, 88 (1965).
3. Yu. I. Smolin and Yu. F. Shepelev, *Izv. Akad. Nauk SSSR Neorg. Mat.* **5**, 1823 (1969).
4. N. A. Toropov and I. A. Bondar, *Izv. Akad. Nauk SSSR, Otd. Khim. Nauk* **4**, 544 (1961); **5**, 739 (1961); **8**, 1372 (1961).
5. N. A. Toropov, F. Ya. Galakhov, and S. F. Konovalova, *Izv. Akad. Nauk SSSR Otd. Khim. Nauk* **4**, 539 (1961); **8**, 1365 (1961).
6. E. K. Keler, N. A. Godina, and E. P. Savchenkov, *Izv. Akad. Nauk SSSR Otd. Khim. Nauk* **10**, 1728 (1961); **10**, 1735 (1961).
7. A. I. Leonov, V. S. Rudenko, and E. K. Keler, *Izv. Akad. Nauk SSSR Otd. Khim. Nauk* **11**, 1925 (1961).
8. R. O. Miller and D. E. Rase, *J. Amer. Ceram. Soc.* **47**, 653 (1964).
9. J. Felsche, *J. Less-Common Metals* **21**, 1 (1970).
10. G. Buisson and C. Michel, *Mater. Res. Bull.* **3**, 193 (1968).
11. Y. I. Smolin and S. P. Tkachev, *Sov. Phys. Crystallogr.* **14**, 14 (1969).
12. J. Felsche, *Naturwiss.*, in press.
13. R. D. Shannon and C. T. Prewitt, *Acta Crystallogr. B* **25**, 925 (1969).
14. D. H. Templeton and C. H. Dauben, *J. Amer. Chem. Soc.* **76**, 5237 (1954).
15. W. L. Wanmaker, W. P. De Graaf, and H. L. Spier, *Physica* **25**, 1125 (1959).
16. I. Warshaw and R. Roy, *in* "Progress in Science and Technology of the Rare Earths," Vol. I, p. 215, Pergamon, New York (1964).
17. A. G. Cockbain and G. V. Smith, *Min. Mag.* **36**, 411 (1968).
18. D. A. Grisafe and F. A. Hummel, *Amer. Min.* **55**, 1131 (1970).
19. H. Schwarz, *J. Inorg. Nucl. Chem. Lett.* **3**, 231 (1967).
20. G. Blasse and J. De Vries, *J. Inorg. Nucl. Chem.* **29**, 1541 (1967).
21. A. S. Posner, A. Perloff, and A. F. Diorio, *Acta Crystallogr.* **11**, 308 (1958).
22. G. J. McCarthy, W. B. White, and R. Roy, *J. Inorg. Nucl. Chem.* **29**, 253 (1967).
23. D. McConnell and M. H. Hey, *Min. Mag.* **37**, 301 (1969).